Effect of resonance production in inclusive reactions and vector-meson-dominance model*

Tateaki Sasaki
Department of Physics, University of Tokyo, Tokyo 113, Japan

Nobuyuki Murai
Department of Physics, McGill University, Montreal 101, Canada
(Received 1 June 1973)

The properties of the inclusive distribution for a resonance-mediated particle are investigated. In particular, vector mesons are considered as examples of the resonances. The longitudinal and transverse momentum distributions, and their dependences on energy and polarization are discussed for the decay products. The actual reaction $pp \to \pi^- X$ is studied within the framework of vector-meson dominance. The assumption of a scaling spectrum for the resonances explains about 50—70% of the observed breaking of the scaling law in this reaction. In the resonance-dominance scheme the resonance multiplicity is much smaller than the final-particle multiplicity. This relates to the slow onset of the scaling limit in exotic inclusive reactions. Further, the relativistic longitudinal phase volume is calculated numerically. The phase-space constraints almost determine the favored distribution.

I. INTRODUCTION

Recently resonance production in multiparticle emission processes has been widely studied experimentally.[1] Because of the complexity in analyzing many-particle states,[2] our knowledge is confined mainly to 6- or fewer-particle final states in the incident energy region below 20 GeV. Nevertheless, we can see that the resonance production is very important quantitatively as well as qualitatively.

On the other hand, several kinds of theoretical models on multiple production suggest that resonances are dominantly produced at high energy. In the multiperipheral model involving π and K exchanges,[3] vector mesons, say ρ and K^*, dominate final states. This feature would be found in Feynman's bremsstrahlung model.[4] In the diffractive-excitation model heavy resonances, or fireballs, are also emitted.[5] One of the authors (T. S.) designed an intuitive model in the context of low-mass-resonance production.[6] In all the above models, save the diffraction-excitation model, resonances are produced not only in the fragmentation region but also in the central region.

Therefore, it is important to investigate the effects of resonance production in addition to those of diffractive dissociation. The main purpose of this paper is to investigate the kinematical effects of vector mesons on pseudoscalar-meson inclusive distributions. To see the effects pertinently, we assume the resonance distribution to be as simple as possible. We do not aim to fit experimental data best. Our study also concerns the thermodynamical model[7] as well as the diffractive-excitation model. In these models an *a priori* form for the π and K distributions from a fireball is assumed. These may be, to some extent, checked by an exact study of resonance decays.

Another motivation for this work derives from the results on inclusive reactions, some of which are summarized below[8]:

(i) In many cases, distributions increase in the central region (the scaling variable $x \simeq 0$) with energy. For example, in the reaction $pp \to \pi^- X$, the distribution at the CERN ISR energy region is 1.7–2.0 times larger than that at 20–30 GeV.

(ii) Spectra in the fragmentation region ($|x|$ is not small) remain unchanged or seem to decrease a little as energy increases. If it is the latter, the hypothesis of limiting fragmentation[9] should be examined again.

(iii) In the central region the slope of pion transverse momentum distribution ($q_\perp^2$ distributions) for $q_\perp^2 \lesssim 0.5$ $(\mathrm{GeV}/c)^2$ increases with energy.

(iv) The particle production ratios K/π and $\bar{p}/\pi$ increase remarkably. In the central region in the CERN ISR experiments the ratio K^-/π^- and the ratio $\bar{p}/\pi^-$ are 2–3 and 3–5 times larger than the corresponding values at 20–30 GeV.[10]

(v) The distribution functions are not factorizable into functions of the individual variables x and $q_\perp$, but show strong correlation.

Many authors have investigated these problems.[11-17] We expect these complicated behaviors to be attributable, to some extent, to resonance

effects. Webber[11] showed, on the basis of the π^--exchange multiperipheral model with the ρ produced dominantly, that the $q_\perp^2$ distribution for a final pion is steeper than for ρ and exhibits the so-called two-slope structure. Cahn[16] examined the consequences of Feynman scaling for photon spectra arising from π° decay at $x=0$. The dip found by him at $q_\perp=0$ has the same kinematical basis as that in π spectra resulting from ρ decay, which is discussed later in this article. Brink *et al.*[18] have made an interesting study of longitudinal distributions in the high-energy limit. Phua and the present authors[19] have studied the reaction $\gamma p \to \pi^- X$ employing the vector-meson-dominance model (VMDM) for the real photon.

The plan of this paper is as follows. In Sec. II we split inclusive distribution into resonance terms and nonresonant ones. Section III concerns analytical study of spectra resulting from vector-meson decay. In Sec. IV numerical investigations are presented for the case of ρ, ω, and K^*. The actual reaction $pp \to \pi^- X$ is analyzed within the framework of vector-meson dominance. In Sec. V we consider the resonance effect on strange-particle or antiproton production in pp collisions, especially the energy dependence. In Sec. VI the resonance distributions are discussed from the kinematical viewpoint of relativistic longitudinal phase volume.

II. FUNDAMENTAL FORMULAS

We consider the following intermediate state in ab collisions:

$$a+b \to C_1+C_2+\cdots+d_1+d_2+\cdots, \tag{2.1}$$

where C_i $(i=1,2,\dots)$ are resonances and d_i $(i=1,2,\dots)$ are particles emitted not through the decay of any resonances. Let us denote by $F_C(\vec{k})$ and $F_d(\vec{q})$ Lorentz-invariant single-particle distributions divided by the total cross section σ for C $(=C_1,C_2,\dots)$ and d $(=d_1,d_2,\dots)$, respectively. That is to say, the production cross sections are related to them by

$$\frac{d\sigma_C}{d^3k}=\sigma\frac{F_C(\vec{k})}{k_0}, \qquad \frac{d\sigma_d}{d^3q}=\sigma\frac{F_d(\vec{q})}{q_0}, \tag{2.2}$$

where $\vec{k}$ and $\vec{q}$ are momenta of C and d, respectively. Further, we introduce the double-particle distribution $F_{CC'}(\vec{k},\vec{k}')$ and $F_{dd'}(\vec{q},\vec{q}')$, which are defined in a similar way to (2.2). Throughout this section C and d (and the primed letters) denote a resonance and a nonresonant particle, respectively.

A resonance C is supposed to decay in the manner

$$C \to n_\alpha d_\alpha + n_\beta d_\beta + \cdots, \tag{2.3}$$

where n_i is the number of d_i $(i=\alpha,\beta,\dots)$. The decay distribution is given by

$$D_C(\vec{k};\vec{q}_\alpha,\vec{q}_\beta,\dots)\frac{d^3q_\alpha}{q_{\alpha 0}}\frac{d^3q_\beta}{q_{\beta 0}}, \tag{2.4}$$

which is normalized to be unity after integration over $\vec{q}_\alpha,\vec{q}_\beta,\dots$. For convenience of discussions below, we define the partially integrated distributions

$$D_C^{(1)}(\vec{k};\vec{q}_\alpha)=n_\alpha\int D_C(\vec{k};\vec{q}_\alpha,\vec{q}_\beta,\dots)\frac{d^3q_\beta}{q_{\beta 0}}\frac{d^3q_\gamma}{q_{\gamma 0}}\cdots, \tag{2.5a}$$

$$D_C^{(2)}(\vec{k};\vec{q}_\alpha,\vec{q}_\beta)=n_\alpha(n_\beta-\delta_{\alpha\beta})\times\int D_C(\vec{k};\vec{q}_\alpha,\vec{q}_\beta,\dots)\frac{d^3q_\gamma}{q_{\gamma 0}}\cdots. \tag{2.5b}$$

It is easy to generalize the above formulas to the case of decay through many channels.

Our next step is to give expressions of the spectrum $f_d(\vec{q})$ for a final particle d by combining the decay distribution (2.4) and F_d, F_C. One of the elements $(d_1,d_2,\dots)$ may coincide with d_α or $d_\beta,\dots$. Accordingly, f_d can be decomposed into two terms, one for resonance-mediated d and the other for the nonresonant d:

$$f_d=f_d^{(1)}+f_d^{(2)}, \tag{2.6}$$

where

$$f_d^{(1)}(\vec{q})=F_d(\vec{q}), \tag{2.7a}$$

$$f_d^{(2)}(\vec{q})=\sum_{C(d)}\int\frac{d^3k}{k_0}F_C(\vec{k})D_C^{(1)}(\vec{k};\vec{q}). \tag{2.7b}$$

Here $C(d)$ means the summation over all resonances that decay into d. The double-particle distribution $f_{dd'}$ consists of five terms as follows:

$$f_{dd'}=f_{dd'}^{(1)}+f_{d(d')}^{(2)}+(1-\delta_{dd'})f_{(d)d'}^{(2)}+f_{dd'}^{(3)}+f_{dd'}^{(4)}, \tag{2.8}$$

where

$$f_{dd'}^{(1)}(\vec{q},\vec{q}')=F_{dd'}(\vec{q},\vec{q}'), \tag{2.9a}$$

$$f_{d(d')}^{(2)}(\vec{q},\vec{q}')=\sum_{C(d')}\int F_{dC}(\vec{q},\vec{k})\,D_C^{(1)}(\vec{k};\vec{q}')\frac{d^3k}{k_0}, \tag{2.9b}$$

$$f^{(2)}_{(d)d'}(\vec{q},\vec{q}')\sum_{C(d)}\int F_{Cd'}(\vec{k},\vec{q}')\,D^{(1)}_{C}(\vec{k};\vec{q})\frac{d^3k}{k_0}\,, \tag{2.9c}$$

$$f^{(3)}_{dd'}(\vec{q},\vec{q}')=\sum_{C(d)}\sum_{C'(d')}\int F_{CC'}(\vec{k},\vec{k}')\,D^{(1)}_{C}(\vec{k};\vec{q})\times D^{(1)}_{C'}(\vec{k}';\vec{q}')\frac{d^3k}{k_0}\frac{d^3k'}{k_0'}\,, \tag{2.9d}$$

$$f^{(4)}_{dd'}(\vec{q},\vec{q}')=\sum_{C(d,d')}\int F_{C}(\vec{k})\,D^{(2)}_{C}(\vec{k};\vec{q},\vec{q}')\frac{d^3k}{k_0}\,. \tag{2.9e}$$

Strictly speaking, (2.8) and (2.9) are valid only when neglecting the interference terms between the resonant and nonresonant amplitudes. Even this simplification, however, yields valuable insight into resonance effects. It should be noted that even if the final states are dominated by resonances, $f^{(3)}_{dd'}$ as well as $f^{(4)}_{dd'}$ contributes to $f_{dd'}$. This means that the assumption of resonance dominance cannot be examined by comparing the single particle $f^{(2)}_{d}$ (assumed to be f_d) with the two-particle spectrum in the invariant-mass plot.

The bulk of the remainder of this section is devoted to expressing the two-particle correlation

$$g_{dd'}=f_{dd'}-f_d f_{d'} \tag{2.10}$$

in terms of $f^{(1)}_{dd'}$, $f^{(1)}_{d}$, and

$$G_{ij}=F_{ij}-F_iF_j\,,$$

$$(i,j)=(C,C'),\ (C,d),\ \text{and}\ (d,d')\,. \tag{2.11}$$

We decompose $g_{dd'}$ into the six terms

$$g_{dd'}=g^{(1)}_{dd'}+g^{(2)}_{d(d')}+(1-\delta_{dd'})g^{(2)}_{(d)d'}+g^{(3)}_{dd'}+f^{(4)}_{dd'}-\delta_{dd'}f^{(1)}_{d}f^{(2)}_{d}\,, \tag{2.12}$$

where

$$g^{(1)}_{dd'}=f^{(1)}_{dd'}-f^{(1)}_{d}f^{(1)}_{d'}\,, \tag{2.13a}$$

$$g^{(2)}_{d(d')}=f^{(2)}_{d(d')}-f^{(1)}_{d}f^{(2)}_{d'}\quad(d\rightleftarrows d')\,, \tag{2.13b}$$

$$g^{(3)}_{dd'}=f^{(3)}_{dd'}-f^{(2)}_{d}f^{(2)}_{d'}\,. \tag{2.13c}$$

The following expressions arise directly from the definitions of g and G, and from (2.5):

$$\int g^{(2)}_{d(d')}\frac{d^3q'}{q_0'}=\sum_{C'(d')}n_{d'}\int G_{dC'}(\vec{q},\vec{k}')\frac{d^3k'}{k_0'}\,, \tag{2.14a}$$

$$\int g^{(2)}_{(d)d'}\frac{d^3q}{q_0}=\sum_{C(d)}n_{d}\int G_{Cd'}(\vec{k},\vec{q}')\frac{d^3k}{k_0}\,, \tag{2.14b}$$

$$\int g^{(3)}_{dd'}\frac{d^3q}{q_0}\frac{d^3q'}{q_0'}=\sum_{C(d)C'(d')}n_dn_{d'}\int G_{CC'}(\vec{k},\vec{k}')\times\frac{d^3k}{k_0}\frac{d^3k'}{k_0'}\,. \tag{2.14c}$$

III. VECTOR-MESON DECAY

Following the general discussions in Sec. II, we develop concrete formulas for the spectrum for a vector meson V, which decays into two spinless particles m and m'. From the empirical point of view,[1] the vector mesons seem to be the most important. For simplicity, suppose that m and m' have an equal mass μ, but are distinguishable from each other. Averaging the m (or m') distribution over the azimuthal angle defined in the helicity frame of V, we have the decay distribution (2.5) in the rest frame of V (see Appendix A):

$$D^{(1)}_{V}(\vec{k}^*,\vec{q}^*)=\frac{1+A\cos^2\theta}{2\pi\eta(1+\frac{1}{3}A)}\,\delta(q_0^{*2}-\tfrac{1}{4}M^2)\,, \tag{3.1}$$

where M is the mass of V,

$$\eta=[1-(2\mu/M)^2]^{1/2}\,, \tag{3.2}$$

and θ is the angle between the momentum $\vec{q}^*$ of m and $\vec{k}^*$ of V. The latter is supposed to be infinitesimal. The parameter A is related to the decay density matrix of V:

$$A=\frac{2d_{00}-d_{11}-d_{-1-1}}{d_{11}+d_{-1-1}}\,. \tag{3.3}$$

The value -1 and ∞ of A correspond to the purely transverse and longitudinal helicity, respectively.

The V rest frame is reached by a pure boost and a rotation from the center-of-mass (c.m.) frame. A short calculation gives the following expression for $D^{(1)}_{V}$ in terms of the momentum $\vec{q}$ of m and $\vec{k}$ of V in the c.m. frame:

$$D^{(1)}_{V}(\vec{k};\vec{q})=\frac{1}{2\pi\eta(1+\frac{1}{3}A)}\left[1+\frac{4A(\vec{k}\cdot\vec{q}\,k_0/|\vec{k}|-|\vec{k}|q_0)}{\eta^2M^4}\right]\times\delta((k_0q_0-\vec{k}\cdot\vec{q})^2-\tfrac{1}{4}M^2)\,. \tag{3.4}$$

Combining (3.4) and (2.7), we have the distribution $f^{(2)}_{m}(\vec{q})$ for m. The parameter A in (3.4), which may depend on $\vec{k}$, is put equal to a constant for simplicity. Then we can integrate $f^{(2)}_{m}$ over the angle of $\vec{k}_\perp$:

$$f_m^{(2)}(\vec{q}) = \frac{1}{\pi\eta(1+\frac{1}{3}A)} \int \frac{k_\perp dk_\perp dk_\parallel}{k_0} F_V(k_\parallel, k_\perp) \left[1 + \frac{4A(\frac{1}{2}k_0 - q_0)^2}{\eta^2(k_\parallel^2 + k_\perp^2)}\right] [(k_\perp q_\perp)^2 - (k_0 q_0 - k_\parallel q_\parallel - \tfrac{1}{2}M^2)^2]^{-1/2}, \tag{3.5}$$

where $k_\parallel$ and $k_\perp$ (or $q_\parallel$ and $q_\perp$) are restricted to the region

$$(k_\perp q_\perp)^2 - (k_0 q_0 - k_\parallel q_\parallel - \tfrac{1}{2}M^2)^2 \geq 0. \tag{3.6}$$

Sometimes we are interested in the total distribution $\bar{f}_m^{(2)}(q_\parallel)$ integrated over $\vec{q}_\perp$:

$$\bar{f}_m^{(2)}(q_\parallel) = \int f_m^{(2)}(\vec{q})\, d^2 q_\perp$$

$$= \frac{2\pi}{\eta(1+\frac{1}{3}A)} \int k_\perp dk_\perp dk_\parallel F_V(k_\parallel, k_\perp)\, (I_0 + 4AI_A/\eta^2), \tag{3.7}$$

with

$$I_0 = (k_\parallel q_\parallel + \tfrac{1}{2}M^2)/(k_\parallel^2 + M^2)^{3/2}, \tag{3.8a}$$

$$I_A = \left[\frac{k_\parallel^2}{k_\parallel^2 + k_\perp^2}(k_\parallel q_\parallel + \tfrac{1}{2}M^2)\left(\frac{\frac{1}{2}k_\parallel - q_\parallel}{k_\parallel^2 + M^2}\right)^2 + \frac{k_\perp^2}{k_\parallel^2 + k_\perp^2} J(k_\parallel, q_\parallel)\right](k_\parallel^2 + M^2)^{-1/2}, \tag{3.8b}$$

where

$$J(k_\parallel, q_\parallel) = \tfrac{5}{2}K^3 - \tfrac{3}{2}K^2 + \tfrac{1}{4}K - \tfrac{3}{2}KL + \tfrac{1}{2}L, \tag{3.9a}$$

$$K = (k_\parallel q_\parallel + \tfrac{1}{2}M^2)/(k_\parallel^2 + M^2), \tag{3.9b}$$

$$L = (q_\parallel^2 + \mu^2)/(k_\parallel^2 + M^2). \tag{3.9c}$$

It is immediately clear from (3.8) that, in the case of $A = 0$, $\bar{f}_m^{(2)}$ is determined by the total distribution $\bar{F}_V(k_\parallel)$, that is, $\bar{f}_m^{(2)}$ does not depend on the detail of the $k_\perp$ distribution.

From the above expressions for $f_m^{(2)}$, we see the following properties:

(i) Compared to F_V, $f_m^{(2)}$ is concentrated more in the central region. This feature is due to sharing of the momentum of V between m and m'. For example, when $M \simeq 2\mu$

$$f_m^{(2)}(\vec{q}) \propto F_V(2\vec{q}). \tag{3.10}$$

(ii) Even if $\bar{F}_V$ scales, $f_m^{(2)}$ deriving from a not flat F_V in x_V does not scale until very high energies. Here we use the scaling variable $x_V = 2k_\parallel/\sqrt{s}$, where $\sqrt{s}$ is the total c.m. energy. To see this clearly, we consider (3.7) for $A = 0$ by taking up the following $\bar{F}_V$ as an example:

$$\bar{F}_V(k_\parallel) = (1 - |x_V|)^\beta, \quad \beta > 0. \tag{3.11}$$

This form is motivated by the limiting fragmentation hypothesis[20] and also agrees in the Regge-pole model. Then

$$\bar{f}_m^{(2)}(q_\parallel) \propto \int_{k_-}^{k_+} \left(1 - \frac{2|k_\parallel|}{\sqrt{s}}\right)^\beta \frac{k_\parallel q_\parallel + \frac{1}{2}M^2}{(k_\parallel^2 + M^2)^{-3/2}} dk_\parallel, \tag{3.12}$$

where

$$k_\pm = (M^2/2\mu^2)\,[q_\parallel \pm \eta(q_\parallel^2 + \mu^2)^{1/2}],$$
$$k_+ \leq \sqrt{s}/2, \quad k_- \geq -\sqrt{s}/2. \tag{3.13}$$

When $q_\parallel = 0$ we have $|k_\pm| = M^2/(2\mu)$. At sufficiently high energy, say $\sqrt{s} \gg \beta M^2/\mu$, we see that

$$\bar{f}_m^{(2)}(0) \propto 1 - c_1/\sqrt{s}, \quad c_1 \geq 0. \tag{3.14}$$

With the same $\bar{F}_V$, the m distribution in the fragmentation region approaches its asymptotic value as

$$\bar{f}_m^{(2)} \propto 1 + c_2/s, \quad c_2 > 0. \tag{3.15}$$

The steeper $\bar{F}_V(k_\parallel)$ is, the larger the energy dependence of $f_m^{(2)}$ is.

(iii) It follows from (3.5) that there must be a correlation between $q_\parallel$ and $q_\perp$ distributions, even if the $k_\perp$ and $k_\parallel$ distributions can be factorized. To obtain a better understanding of this feature, we rewrite (3.5) for $A = 0$ as

$$f_m^{(2)}(\vec{q}) = [\pi\eta(q_\parallel^2 + \mu^2)^{1/2}]^{-1} \times \int_{k_-}^{k_+} dk_\parallel \int_0^\pi d\zeta \times F(k_\parallel, (K^2 - k_\parallel^2 - M^2)^{1/2}), \tag{3.16}$$

where

$$K = \{q_0(k_\parallel q_\parallel + \tfrac{1}{2}M^2) + q_\perp \mu[(k_+ - k_\parallel)(k_\parallel - k_-)]^{1/2}\cos\xi\}(q_\parallel^2 + \mu^2)^{-1} \tag{3.17}$$

When $|q_\parallel| \gg q_\perp$ and μ, $K^2 - k^2$ is proportional to $q_\perp^2$. Therefore, the $q_\perp$ distribution is regular. If $M \gg 2\mu$ and $F_V(\vec{k})$ is a decreasing function of $|k_\parallel|$ and $|k_\perp|$, $f_m^{(2)}$ has a dip at $\vec{q} \sim 0$. This feature can be easily seen by examining the $q_\perp$ dependence of $K^2 - k_\parallel^2 - M^2$ for small $q_\parallel$. When $\vec{q} = 0$, F_V at

$|\vec{k}| = M[(M/2\mu)^2 - 1]$ contributes to $f_m^{(2)}$. This very large value of $|\vec{k}|$ leads to very small F_V. If $M \sim 2\mu$, such a dip does not appear.

We shall postpone the discussion of the two-particle distributions and correlations to Ref. 21.

IV. NUMERICAL INVESTIGATIONS AND VECTOR-MESON-DOMINANCE MODEL

From the formulas presented in Sec. III it is rather complicated to see analytically the amount of resonance effects on the distributions of resonance-mediated particles. It is worthwhile to investigate them numerically by assuming adequate spectra for the resonances. First we shall compute the distribution for π produced through the decay of ρ and ω. Next we shall interpret the actual reaction $pp \to \pi^- X$ in the framework of vector-meson dominance.

We present formulas for calculating the distributions for π resulting from the decay of ρ, ω, and K^*, and for K resulting from K^* and ϕ, in Appendix B by modifying (3.4) etc. The masses of ρ, ω, K^*, π, and K are set to be 0.76, 0.784, 0.890, 0.140, and 0.495 (in GeV units), respectively. The widths are 0.135 for ρ and 0 for others.

A. $\rho \to 2\pi$, $\omega \to 3\pi$

We assume scaling and factorized distributions for vector mesons:

$$F_V(k_\parallel, k_\perp) = F_\parallel(x_V) F_\perp(k_\perp). \tag{4.1}$$

The function $F_\parallel$ is assumed to be of the form (3.11), and $F_\perp$ is chosen to be

$$F_\perp(k_\perp) = \exp(-c k_\perp^2), \tag{4.2}$$

where $\beta = 2.2$ and $c = 5.0$ $(\mathrm{GeV}/c)^{-2}$. The Gaussian form (4.2) is assumed so as to see clearly the two-slope structure in the transverse-momentum distribution plotted versus $q_\perp^2$ for π.

Figure 1 shows the longitudinal momentum distribution for π resulting from ρ decay. As the energy of the incident proton in the laboratory system increases from 12.0 GeV first to 28.5 and then to 1500 GeV, the distribution decreases by 9% and 18%, respectively, at $x = 0.5$, while at $x = 0$ it increases by 15% and 50%, respectively. Note the considerable change of the spectrum as the energy increases, as well as its slow pace to the asymptotic region, in particular, in the central region. From the viewpoint of fireball production, Jacob *et al.*[5] and Ranft[14] also showed the increase in the central region. It was assumed that heavier fireballs were produced with increasing energy. However, the distribution in the fragmentation region does not decrease in their models.

The shape of the x distribution depends considerably on A. However, only the behavior at $x \sim 0$ is interesting and the steepness of the distributing depending on A is useless in determining A, since A and β are correlated. It seems that, in the resonance-dominance scheme, $A = -1$ is rather unfavorable.

Figure 2 displays the transverse distribution for π resulting from ρ decay. One of the prominent features is a deep dip at $\vec{q} = 0$. Experimental check of it would be one of the crucial tests in the choice among various resonance-dominance models. It is interesting to note that an e^--removed π^- distribution at CERN ISR energy[8] shows the dip structure, although only one point of the data falls off the regular spectrum. It should be mentioned that Webber's results[11] did not provide us such a dip in the two-slope structure.

Note that the appearance of the dip depends

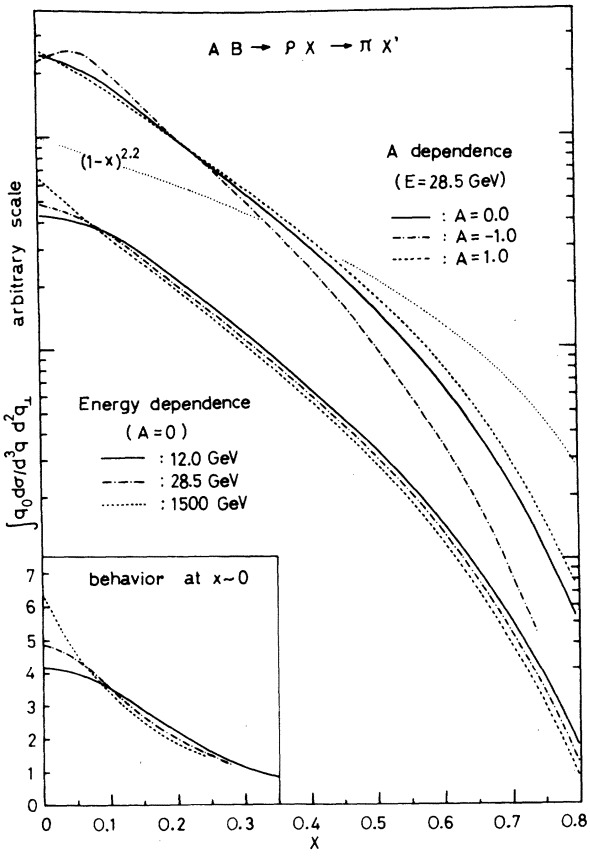

FIG. 1. The energy and A dependences of invariant longitudinal distributions of π produced through ρ. The ρ distribution is assumed to scale, which is also shown for comparison. A is related to the polarization of ρ [see Eq. (3.3)].

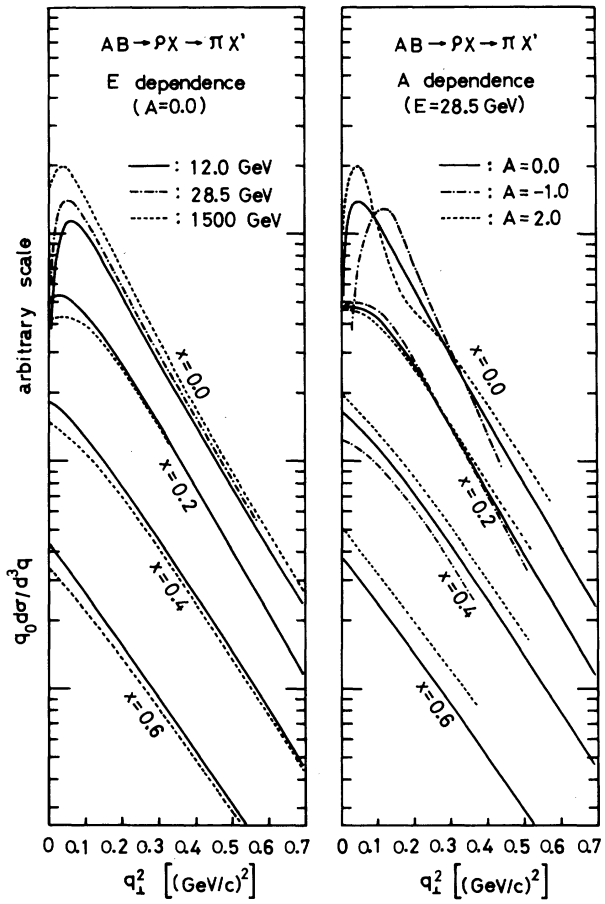

FIG. 2. The energy x and A dependences of invariant transverse-momentum distributions of π produced through ρ. The ρ distribution is assumed to be factorized with respect to variables $k_\parallel$ and $k_\perp$.

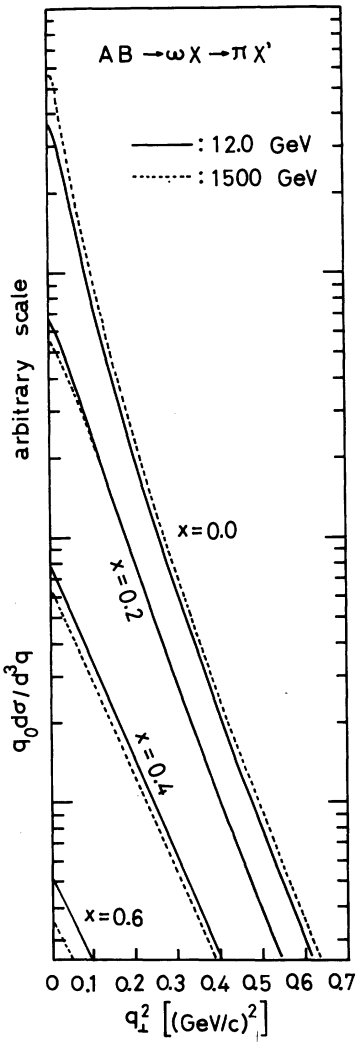

FIG. 3. The invariant transverse-momentum distribution of π produced through ω. The ω distribution is assumed to be the same as ρ distribution.

on both the mass ratio $2\mu/M$ and the decay mode. For comparison, we show the $q_\perp^2$ distribution for π's coming from ω decay in Fig. 3. There appears a sharp peak instead of a dip. Thus, there is a possibility that the dip found in the ρ decay is filled up by other resonances. Further, it should be noted that the dip becomes shallower as the energy increases.

It can be seen in Fig. 2 that, aside from the dip, the slope is steeper for smaller $|x|$ inspite of the factorization (4.1). Besides, near $x=0$, the $q_\perp^2$ distribution shows shrinkage with increasing energy. These features are also suggested by experiment.

The slope at $x=0$ is less dependent on c in (4.2) as compared to that at intermediate x: It is about 6.8 $(\mathrm{GeV}/c)^{-2}$ for $c=5.0$ $(\mathrm{GeV}/c)^{-2}$, while 5.0 $(\mathrm{GeV}/c)^{-2}$ for $c=2.5$ $(\mathrm{GeV}/c)^{-2}$ in the region $q_\perp^2=0.2$–0.3 $(\mathrm{GeV}/c)^2$.

The $q_\perp^2$ spectrum indicates a rather strong A dependence at $x=0$. As far as we are concerned with single-particle distributions, the experimental determination of A would be possible only through the observation of this behavior. It is plausible to say that the non-negative A is favored by the present experiments.

B. $pp\to\pi^- X$

Now we explore the actual reaction $pp\to\pi^- X$ taking account of K^* and ω as well as ρ. There are two reasons to include K^* and ω: The first is to see what amount of the dip at $q_\perp\sim 0$ is filled up. Secondly, the K/π ratio $R(K/\pi)$ depends strongly on energy and becomes pretty large at CERN ISR energy. For simplicity, we ignore the ϕ meson.

Up to now we have adopted functions which scale

completely. However, the remarkable energy dependences of $pp(K^-)$ and $pp(\bar{p})$ etc. are not compatible with a scaling function for K^*. We will discuss this unfortunate situation in Sec. V. Our procedure for calculation is the following:

(i) We multiply an energy-dependent factor by the scaling distribution (3.11); that is, for a resonance V the distribution reads

$$\gamma_V(s)F_V(x) \text{ with } \beta = 2.2 . \tag{4.3}$$

(ii) We impose on γ_V the condition that the total contribution of ρ, ω, and K^* should scale. Under the assumption that each component of an isomultiplet is produced with an equal weight, the condition is expressed as

$$\tfrac{2}{3}\gamma_\rho + \gamma_\omega + \tfrac{1}{3}\gamma_{K^*} = \text{constant} \tag{4.4}$$

irrespective of s. However, the ratio $R(K/\pi)$ is energy-dependent and is given by experiments:

$$R(K^-/\pi^-) = \frac{\frac{1}{4}\gamma_{K^*}}{\frac{2}{3}\gamma_\rho + \gamma_\omega + \frac{1}{3}\gamma_{K^*}} . \tag{4.5}$$

Finally, we regard $\gamma_\omega/\gamma_\rho$ as a parameter.

(iii) Since $F_\perp(k_\perp)$ given by (4.2) cannot reproduce the experimental $q_\perp{}^2$ distribution for $q_\perp{}^2 \gtrsim 0.5$ $(\text{GeV}/c)^2$, we shall modify $F_\perp(k_\perp)$ for the ρ meson as

$$F_\perp(k_\perp) = 0.4\exp(-5.0k_\perp{}^2) + 0.6\exp(-2.5k_\perp{}^2) .$$

The π^- distribution obtained in the framework (i)–(iii) is quite similar to that resulting from the completely scaling resonance spectra. Thus we may call (4.3) quasi-scaling spectrum.

In Fig. 4 we illustrate a comparison of the VMDM with the experiment at 28.5 GeV, with $\gamma_\omega/\gamma_\rho$ set equal to 0.1. The energy-independent normalization is obtained by fitting the observed π^- distribution at $q_\perp = 0.2$ GeV/c and 28.5 GeV (Fig. 5). The theoretical $q_\perp{}^2$ distribution at $q_\perp{}^2 = 0.2$–0.3 $(\text{GeV}/c)^2$ has a smaller slope than the experimental one. The behavior at $q_\perp{}^2 \sim 0$ is much improved, but still far from the experimental data.

In Fig. 5 the calculated energy dependence of the calculated x distribution for $0 < x \lesssim 0.3$ is compared with the observed one. The value of $R(K^-/\pi^-)$ at 12.0, 28.5, and 1500 GeV are put equal to be 0.023, 0.038, and 0.085, respectively.[10] For $q_\perp = 0.2$ GeV/c, our result is rather consistent with the e^--removed data, although other ISR data are systematically larger than the theoretical curve. The curves calculated at $q_\perp = 0.4$ GeV/c are above the observed ones. Next we turn our attention to a crossover between two curves at 28.5 GeV and ISR energy. It is shown in Fig. 5 that the theoretical crossover point is at $x \sim 0.08$, while the experimental one is at $x \sim 0.17$ though yet unconfirmed. We compared the theoretical curves with the spectra for $pp \to \pi^+X$,[8] which is known to be less energy dependent than that for $pp \to \pi^-X$, and found much better agreement between the model and the experiments, although at $q_\perp = 0.4$ GeV/c, the experimental crossover point is still larger than the calculated one.

In conclusion, it is plausible to say that the effect of resonance, whose distribution already scales or quasi-scales, explains the considerable part of observed breaking of the scaling law in $pp \to \pi^\pm X$ in the energy region 30–1500 GeV.

The scaling hypothesis should, therefore, be reviewed by taking the resonance effects into consideration.

V. EXOTIC INCLUSIVE SPECTRA

In this section we shall discuss the energy dependence of the spectrum for a strange particle or an antibaryon in pp collisions. Their

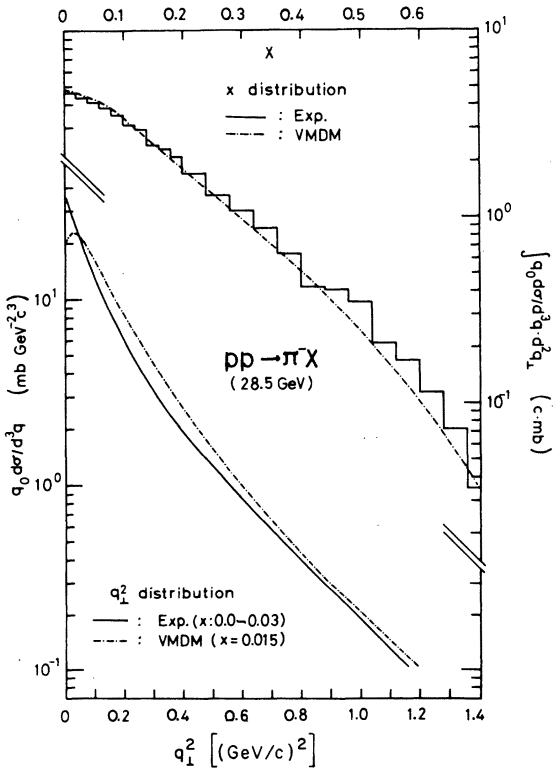

FIG. 4. Comparison of VMDM with the observed spectrum of $pp \to \pi^-X$ at 28.5 GeV. The theoretical curves are not the best fit. The parameters are set as $\gamma_\omega/\gamma_\rho = 0.1$ and $R(K^-/\pi^-) = 0.038$. The data are taken from Ref. 8(c).

distributions change considerably even at the incident laboratory energy $E_{lab} = 1000$ GeV. On the other hand, an estimate[12] in the multiperipheral model with π and K directly produced indicates that these distributions should scale already at $E_{lab} = 40$–50 GeV. We shall point out a possibility that this discrepancy can be removed by the resonance effect, if the final produced particles come dominantly from resonances.

In the multiperipheral model, the quantum number of the final particles are affected by those of the initial particles through a single chain of exchanged particles. We denote by α the representative number of particles counted from each end of the chain, which are under the influence of the incident particles. The average multiplicity may be expressed by

$$\langle n \rangle = c \ln E + d , \tag{5.1}$$

where E is the laboratory energy. Exotic inclusive reactions would scale only after the number of produced particles becomes larger than 2α. Here we call the inclusive reaction $AB \to CX$ exotic if $(A\bar{C})$ and/or $(B\bar{C})$ are exotic; otherwise, it is nonexotic. We define the asymptotic energy as that in which the particle production ratios are independent of the energy. Let E_1 denote the asymptotic energy in the absence of resonance formation in the final state. Then

$$c \ln E_1 + d \sim 2\alpha . \tag{5.2}$$

On the other hand, in the resonance-dominance scheme, the scaling region above E_2 is given by the equation

$$c \ln E_2 + d \sim 2\gamma\alpha , \tag{5.3}$$

where γ is the mean number of particles produced from a single resonance. If $E_1 \sim 40$ GeV and $\gamma \sim 2$, we have $E_2 \sim 1000$ GeV. This simple calculation demonstrates that resonances, if they are produced abundantly, can alter the energy dependence of original distribution $F(\vec{k})$ drastically. Perhaps, this is one of the most important effects of resonance production.

Thus we make a conjecture with relation to the scaling law: Resonance dominance, or clustering in the final state, implies that the original (resonance) distributions for exotic inclusive reactions would not scale below quite high energy, while those for nonexotic reactions scale early.

VI. KINEMATICAL STUDY OF RESONANCE DISTRIBUTIONS

So far we have discussed mainly the kinematical effects of mediating resonances, assuming particular forms of the resonance spectra. To understand these spectra themselves, we shall calculate them from the relativistic phase volume. We start with introducing our terminology and notation. Note that the notation in this section is independent of that used so far. We call a single-particle distribution with a fixed number of final particles a partial-inclusive distribution. We denote the two-dimensional momenta of the whole system and a particle i in the final state by $P = (P_0, P_\parallel)$ and $p_i = (p_{i0}, p_{i\parallel})$, respectively. Our definition of the two-dimensional scalar product is $ab = a_0 b_0 - a_\parallel b_\parallel$. Further, m, $p_\perp$, and Δ designate mass, transverse momentum, and longitudinal mass $(\Delta^2 = p_\perp^2 + m^2)$, respectively.

We define the relativistic longitudinal phase volume as follows:

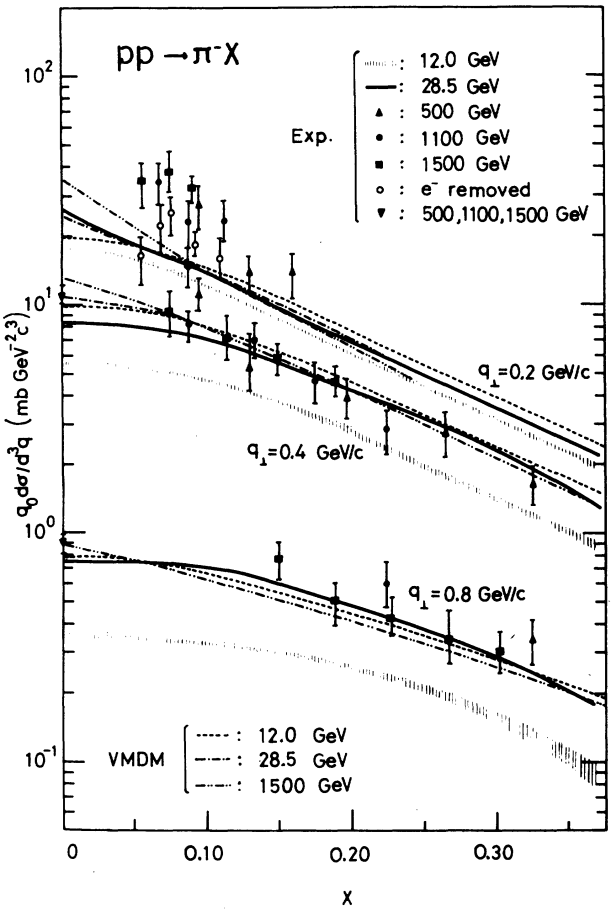

FIG. 5. Comparison of VMDM with experiments in $|x| \lesssim 0.3$. Theoretical curves are not the best fit. Normalization is made so that the theoretical curve fits the experiment for $q_\perp = 0.2$ GeV/c at 28.5 GeV best. $\gamma_\omega/\gamma_\rho = 0.1$ for all energies. $R(K^-/\pi^-)$ at 12.0, 28.5, and 1500 GeV are set 0.023, 0.038, and 0.085, respectively. The data are taken from Ref. 8(g).

$$\Omega_N(P)=g^N\int_{-\infty}^{\infty}\prod_{i=1}^{N}[dp_{i0}\,dp_{i\parallel}\,\delta(p_i{}^2-\Delta_i{}^2)\theta(p_{i0})]\,\delta^2\Big(P-\sum_{i=1}^{N}p_i\Big). \tag{6.1}$$

For $N=2$ and 3, the integration can be performed:

$$\Omega_2(W,0)=g^2/\{[W^2-(\Delta_1+\Delta_2)^2]\,[W^2-(\Delta_1-\Delta_2)^2]\}^{1/2}, \tag{6.2}$$

$$\Omega_3(W,0)=\frac{2g^3F(\frac{1}{2}\pi,k)}{(W+\Delta_1+\Delta_2+\Delta_3)\,(W+\Delta_1-\Delta_2-\Delta_3)\,(W+\Delta_2-\Delta_1-\Delta_3)\,(W+\Delta_3-\Delta_1-\Delta_2)} \tag{6.3}$$

where $W=(P^2)^{1/2}$ and

$$F(\phi,k)=\int_0^{\phi}d\theta(1-k^2\sin^2\theta)^{1/2}, \tag{6.4}$$

with

$$k^2=\frac{[W^2-(\Delta_1+\Delta_2+\Delta_3)^2]\,[W^2-(\Delta_1-\Delta_2-\Delta_3)^2]\,[W^2-(\Delta_2-\Delta_3-\Delta_1)^2]\,[W^2-(\Delta_3-\Delta_1-\Delta_2)^2]}{(W+\Delta_1+\Delta_2+\Delta_3)^2\,(W+\Delta_1-\Delta_2-\Delta_3)^2\,(W+\Delta_2-\Delta_3-\Delta_1)^2\,(W+\Delta_3-\Delta_1-\Delta_2)^2}. \tag{6.5}$$

For $N\geq 4$ the integration in (6.1) cannot be done analytically. We adopt the central-limit theorem in probability theory to obtain an approximate formula for (6.1). The derivation is not shown here because of its tediousness, but for the details the reader can consult Ref. 22. Before writing down the formula, we define some functions employed: $K_i(z)$ is the ith-order modified Bessel function of the second kind. It is convenient to introduce the function

$$R(z)=zK_1(z)/K_0(z), \tag{6.6}$$

the new variables $z_i=\beta\Delta_i$ ($i=1,2,\ldots,N$, β is a parameter), and the functions

$$f_2(\beta)=-\sum[R(z_i)]^2+\sum R(z_i)+\sum z_i{}^2, \tag{6.7a}$$

$$f_3(\beta)=-2\sum[R(z_i)]^3+3\sum[R(z_i)]^2+2\sum[(z_i{}^2-1)R(z_i)]-\sum z_i{}^2, \tag{6.7b}$$

$$f_4(\beta)=-6\sum[R(z_i)]^4+12\sum[R(z_i)]^3+\sum[(8z_i{}^2-11)R(z_i)^2]+\sum[(6-8z_i{}^2)R(z_i)]+\sum(3z_i{}^2-2z_i{}^4). \tag{6.7c}$$

Now we can give the approximate formula for (6.1):

$$\Omega_N(P)=\Omega_N^{(0)}(W;\beta)\,[1+G_N(\beta)+O(N^{-3/2})], \tag{6.8}$$

where

$$\Omega_N^{(0)}(W;\beta)=\frac{\prod_{i=1}^{N}K_0(\beta\Delta_i)}{2\pi[f_2(\beta)W/\beta^3]^{1/2}}\exp(\beta W). \tag{6.9}$$

The parameter β is given as a solution to the equation

$$W=\frac{1}{\beta}\sum_{i=1}^{N}R(\beta\Delta_i). \tag{6.10}$$

The second term inside the square brackets of (6.8) is the following function:

$$G_N(\beta)=\tfrac{1}{8}\Big[\frac{f_4}{f_2{}^2}-\frac{2(f_3-2f_2-2\beta W)}{f_2\beta W}+\frac{3(f_2+\beta W)}{(\beta W)^2}\Big]-\tfrac{1}{24}\Big[\frac{5f_3{}^2}{f_2{}^3}-\frac{6f_3(f_2+\beta W)}{f_2{}^2\beta W}+\frac{9(f_2+\beta W)^2}{f_2\beta^2W^2}\Big]. \tag{6.11}$$

To see the accuracy, we apply the formula (6.8) to the case of $N=2,3$ and compare the values obtained from it with the exact ones in Table I. The agreement is very good. It is expected from this result that the error in the statistical approximation lies around 1–4% for $N=4$ and is

TABLE I. Relativistic longitudinal phase volumes of N-body systems for $N=2$ and 3. The values in the left-hand columns are by the exact formula and those in the right-hand columns are by the approximate one. The c.m. total energy is $W=\sqrt{P^2}$. In the table $a(-b)$ means $a\times 10^{-b}$.

W (GeV)	$N=2$		$N=3$	
	Exact	Approx.	Exact	Approx.
2.856	2.305(−2)	2.306(−2)	3.605(−2)	3.645(−2)
4.827	7.225(−3)	6.676(−3)	1.614(−2)	1.604(−2)
8.157	2.446(−3)	1.986(−3)	7.017(−3)	6.760(−3)
13.79	8.469(−4)	5.625(−4)	2.962(−3)	2.727(−3)
23.30	2.954(−4)	1.419(−4)	1.218(−3)	1.055(−3)
39.37	1.033(−4)	2.696(−5)	4.909(−4)	3.922(−4)
66.54	3.614(−5)	2.251(−7)	1.944(−4)	1.400(−4)

still small for $N>5$.

Figure 6 shows the phase volume with the same parameters as in Table I. We employ the exact formula for $N=2$ and 3 and the approximate one for $N>4$.

Now we are in a position to consider the kinematical constraints from the phase volume on the inclusive distribution for a resonance. Suppose that the quantity y is a function of p_i $(i=1,\ldots,N)$; i.e., $y=h(p_1,p_2\ldots,p_N)$. Then we can give the distribution for y

$$H(y)=\int \delta[y-h(p_1,p_2,\ldots,p_N)] \times\rho_N(P;p_1,p_2,\ldots,p_N)\prod_{i=1}^{N}(d^2p_i), \quad (6.12)$$

where the normalized distribution function ρ_N of N particles is

$$\rho_N(P;p_1,p_2,\ldots,p_N)=\frac{g^N}{\Omega_N(P)}\,\delta^2\Big(P-\sum_{i=1}^{N}p_i\Big) \times\prod_{i=1}^{N}[\,\delta(p_i^2-\Delta_i^2)\theta(p_{i0})]\,. \quad (6.13)$$

By putting $y=p_N=p$ in (6.12), a simple manipulation gives the following partial-inclusive distribution which results only from the phase volume:

$$\frac{d\sigma_N}{dp_{\parallel}}=\frac{g\Omega_{N-1}(P')}{2p_0\Omega_N(P)}\,, \quad (6.14)$$

with

$$P'^2=(P-p)^2=P^2+\Delta^2-2P\cdot p\,. \quad (6.15)$$

The longitudinal phase volume behaves at high energy as $\Omega_N(W,0)$ and

$$\Omega_N(W,0)\propto(\ln W^2)^{N-1}/W^2\,. \quad (6.16)$$

Therefore, the maximum point of the distribution (6.14) spreads out in rapidity space as energy increases.[23] This does not correspond to the realistic case. In order to circumvent this difficulty, we shall take account of the leading-particle effects. It is known empirically that, in many cases, the so-called leading particles carry away a large fraction of the available energy. In practice, therefore, (6.13) should be modified as follows:

$$\rho_n(P;p_A,p_B,p_1,\ldots,p_n) =\frac{F(p_A,p_B)}{C}\,\delta^2\Big(P-p_A-p_B-\sum_{i=1}^{n}p_i\Big) \times\prod_{i=A,B,1}^{n}[\,\delta(p_i^2-\Delta_i^2)\theta(p_{i0})]\,. \quad (6.17)$$

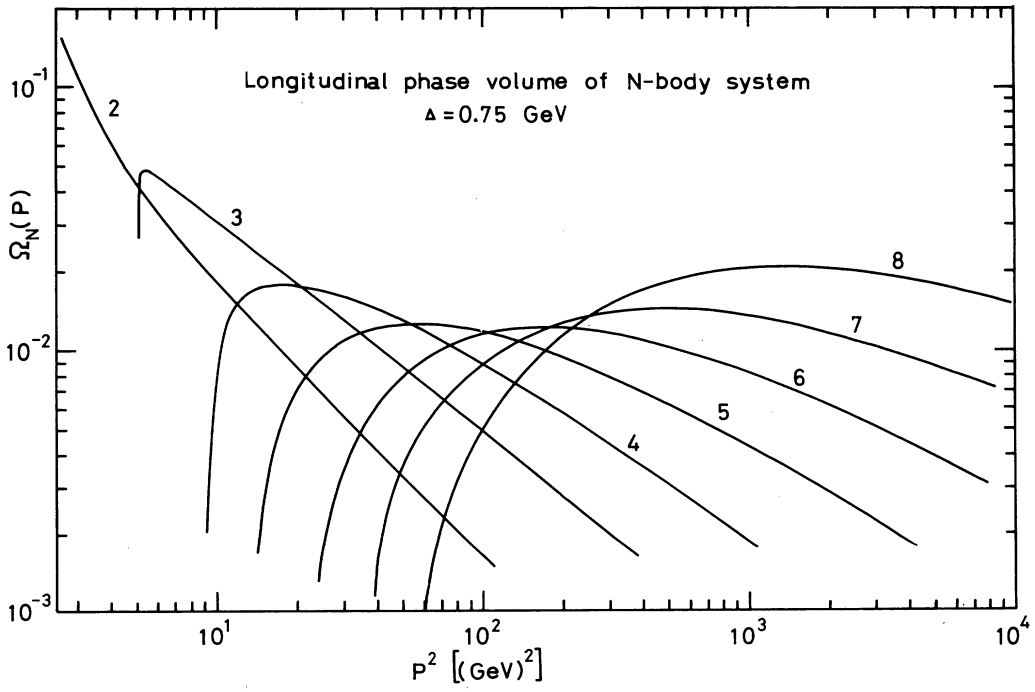

FIG. 6. Relativistic longitudinal phase volume, which is exact for $N=2$ and 3 and approximate for $N>4$. The parameters are $g=0.4$ and $\Delta_i=\Delta=0.75$ GeV.

Here A and B are leading particles and C is a normalization factor. We invoke the general formula (6.12) to obtain the relation between $F(\rho_A, \rho_B)$ and the two-particle distribution for A and B:

$$\frac{d\sigma_n(p_A,p_B)}{dp_{A\parallel}dp_{B\parallel}} = \frac{F(p_A,p_B)}{4Cp_{A0}p_{B0}}\Omega_n(P-p_A-p_B). \quad (6.18)$$

Combining (6.12), (6.17), and (6.18), we have the following partial-inclusive distribution with leading particle effect:

$$\frac{d\sigma_n^{AB}}{dp_\parallel} = \frac{1}{2p_0}\int \frac{d\sigma_n(p_A,p_B)}{dp_A dp_B} \times \frac{\Omega_{n-1}(P-p_A-p_B)}{\Omega_n(P-p_A-p_B)}\, dp_{A\parallel}dp_{B\parallel}. \quad (6.19)$$

In this paper the leading-particle distribution is assumed to be as follows:

$$\frac{d\sigma_n(p_A,p_B)}{dp_{A\parallel}dp_{B\parallel}} = 1/(p_\parallel^{\text{c.m.}})^2 \quad \text{when} \quad p_{A\parallel} \le 0 \quad \text{and} \quad p_{B\parallel} \ge 0$$
$$= 0 \quad \text{otherwise}, \quad (6.20)$$

where $p_\parallel^{\text{c.m.}}$ is the momentum of an incident particle in the c.m. frame.

In Fig. 7 are shown the invariant partial-inclusive distribution $p_0 d\sigma_n(p)/dp_\parallel$ without the leading-particle effect and $p_0 d\sigma_n^{AB}(p)/dp_\parallel$ with the effect, where we set $\Delta_i = \Delta = 0.75$ GeV and $\Delta_A = \Delta_B = 0.95$ GeV. With the choice of $\Delta_i = \Delta = 0.35$ GeV and $\Delta_A = \Delta_B = 0.95$ GeV, we have also calculated the kinematical distributions (6.19) for a nonresonant particle directly emitted. It is found that they are not very different from those for a resonance at CERN ISR energy, provided that n is not large. In this sense, the constraints from the energy-momentum conservation are not sensitive to the mass of a produced particle. In contrast, as shown in the preceding sections, the distribution function for a final particle is quite sensitive to whether resonances are dominantly produced or not, since it changes appreciably through the decay processes.

It is of interest to compare the kinematical spectra (6.14) and (6.19) with the favored [$\beta = 0$ in (3.11)] and disfavored ($\beta > 0$) distributions, respectively. There is fair agreement for the favored one. However, $p_0 d\sigma_n^{AB}(p)/dp_\parallel$ is considerably flatter than the disfavored spectrum.

ACKNOWLEDGMENTS

The authors would like to thank Professor B. Margolis, Professor H. Miyazawa, and Professor H. Sugawara for encouragement. Thanks are also due to Professor M. Koshiba for critical comments. They are very grateful to Dr. S. Chada for a careful reading of the manuscript.

APPENDIX A

A decay angular distribution for a vector meson can be expressed in terms of the density matrix. We designate momenta of an incident particle and the produced vector meson V by $\vec{p}$ and $\vec{k}$, respectively. The z axis is chosen in the direction of $\vec{k}$. The y axis is normal to the production plane: $\vec{y} \propto \vec{p}$ and $\vec{k}$, respectively. The z axis is chosen in the direction of $\vec{k}$. The y axis is normal to the production plane: $\vec{y} \propto \vec{p} \times \vec{k}$. In the rest frame of V, θ and ϕ are defined as the polar and azumuthal angles of the momentum $\vec{q}$ of one of the decay products:

$$\cos\theta = \vec{q}\cdot\vec{z}/|\vec{q}|,$$
$$\cos\phi = \vec{y}\cdot(\vec{z}\times\vec{q})/|\vec{z}\times\vec{q}|. \quad (A1)$$

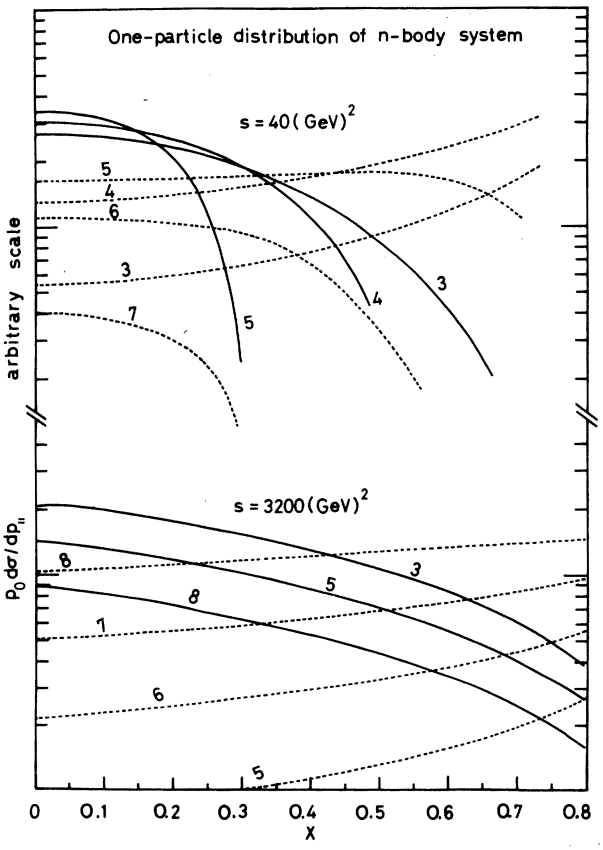

FIG. 7. Invariant semi-inclusive distribution function of resonance with the leading-particle effect (solid curves) and without the leading-particle effect (dotted curves) for $s = 40$ and 3200 GeV^2. For the leading-particle distribution see Eq. (6.20) in the text. The parameters are $g = 0.4$, $\Delta_i = \Delta = 0.75$ GeV, and $\Delta_A = \Delta_B = 0.95$ GeV.

The decay angular distribution of V in the rest frame is given by

$$W(\theta,\phi)=\sum_{\lambda\lambda'}\langle\theta,\phi\,|\,N\,|\,\lambda\rangle\, d_{\lambda\lambda'}\langle\lambda'\,|\,N^{\dagger}\,|\,\theta,\phi\rangle\,, \qquad \text{(A2)}$$

where N is the decay amplitude, $d_{\lambda\lambda'}$ is the density matrix, and λ or λ' denotes the helicity state of V. The explicit form of (A2) is[24]

$$W(\theta,\phi)=(3/4\pi)\left[\tfrac{1}{2}(d_{11}+d_{-1\,-1})\sin^2\theta+d_{00}\cos^2\theta+(1/\sqrt{2})\,(-\mathrm{Re}d_{10}+\mathrm{Re}d_{-10})\sin2\theta\cos\phi\right.$$
$$\left.+(1/\sqrt{2})\,(\mathrm{Im}d_{10}+\mathrm{Im}d_{-10})\sin2\theta\sin\phi-\mathrm{Re}d_{1\,-1}\sin^2\theta\cos2\phi+\mathrm{Im}d_{1\,-1}\sin^2\theta\sin2\phi)\right]. \qquad \text{(A3)}$$

Integrating (A3) with respect to ϕ, we have

$$\int W(\theta,\phi)\,d\phi = \tfrac{3}{4}(d_{11}+d_{-1\,-1})\left(1+\frac{2d_{00}-d_{11}-d_{-1\,-1}}{d_{11}+d_{-1\,-1}}\cos^2\theta\right) \qquad \text{(A4)}$$

The above equation (A4) leads to (3.2) and (3.3).

APPENDIX B

We write down formulas for the π and the K distributions in terms of the spectra for ρ, K^*, ω, and ϕ in the following four subsections, respectively. For convenience, we denote the distribution function in (3.4) by $f(q;M,\mu)$. Let masses of ρ, K^*, ω, ϕ, π, and K be M_ρ, M_K, M_ω, M_ϕ, μ_π, and μ_K, respectively.

1. $\rho\to 2\pi$

In this case we have only to modify (3.4) and (3.6) by including the effect of ρ width. Thus, we obtain the π distribution

$$f_{(\rho\to\pi)}(\vec{q})=\int\frac{\Gamma/2\pi}{(M-M_\rho)^2+\frac{1}{4}\Gamma^2}\,f(\vec{q};M,\mu_\pi)\,dM\,, \qquad \text{(B1)}$$

where Γ is the width of ρ. It is easy to obtain a similar formula for $\bar{f}$.

2. $K^*\to K\pi$

First we consider the π distribution. In the K^* rest frame the energy of π is a constant, which is designated by q^*. We can regard this pion as a decay product of V with the mass $2q^*$, which decays into 2π. The distribution function of this virtual particle V must be

$$(M_K/M)^2F_K((M_K/M)k_{\parallel},(M_K/M)k_{\perp})\,, \qquad \text{(B2)}$$

with

$$M=2q^*=2(M_K^2+\mu_\pi^2-\mu_K^2)/M_K\,. \qquad \text{(B3)}$$

Hence

$$f_{(K^*\to\pi)}(\vec{q})=f'\left(\vec{q};\frac{2(M_K^2+\mu_\pi^2-\mu_K^2)}{M_K},\ \mu_\pi\right) \qquad \text{(B4)}$$

where f' is given by the replacement of F_V in (3.4) with (B2). Similarly, we have

$$f_{(K^*\to K)}(\vec{q})=f'\left(\vec{q};\frac{2(M_K^2+\mu_\pi^2-\mu_K^2)}{M_K},\ \mu_K\right) \qquad \text{(B5)}$$

3. $\omega\to 3\pi$

Although, in this case, the decay distribution may depend on the dynamics, we take account only of the phase-space constraints. That is, the decay distribution for a resultant π is expressed in the ω rest frame as

$$d\sigma^{(0)}(\vec{q};\omega\to 3\pi)\propto\frac{d^3q}{q_0}\int\delta^4(q+q'+q''-p_\omega)\times\frac{d^3q'}{q_0'}\,\frac{d^3q''}{q_0''}\,, \qquad \text{(B6)}$$

with $p_\omega=(M_\omega,\vec{0})$. A comparison (B6) with experiments shows that our ignorance of the dynamics is not crucial. Including the normalization, the explicit form of $d\sigma^{(0)}$ reads

$$d\sigma^{(0)}=\left(1-\frac{4\mu_\pi^2}{M_\omega^2-2M_\omega q_0+\mu_\pi^2}\right)^{1/2}\frac{d^3q}{(cq_0)}\,, \qquad \text{(B7)}$$

where the constant c is taken as

$$c=\int\left(1-\frac{4\mu_\pi^2}{M_\omega^2-2M_\omega q_0+\mu_\pi^2}\right)^{1/2}\frac{d^3q}{q_0}\,. \qquad \text{(B8)}$$

With $M_0=(M_\omega^2-3\mu^2)/M_\omega$, (B7) can be rewritten as

$$d\sigma^{(0)}=\frac{\pi}{c}\int_{2\mu_\pi}^{M_0}dMM\eta\left(1-\frac{4\mu_\pi^2}{M_\omega^2-M_\omega M+\mu_\pi^2}\right)^{1/2}\times\frac{\delta(q_0^2-\frac{1}{4}M^2)}{2\pi\eta}\,. \qquad \text{(B9)}$$

Comparing (B9) with (3.1) one can consider the $\omega\to 3\pi$ decay as a two-body decay of a virtual par-

ticle with the mass M, which is distributed with the weight

$$(M^2-4\mu_\pi{}^2)^{1/2}\left[1-4\mu\pi/(M_\omega{}^2-M_\omega M+\mu_\pi{}^2)\right]^{1/2}$$

in the region $2\mu_\pi \leq M \leq M_0$ and decays into 2π. Thus neglecting the width of ω, we have the π distribution

$$f_{(\omega\to\pi)}(\vec{q})=\frac{\pi}{c}\int_{2\mu}^{M_0} dM\left[(M^2-4\mu_\pi{}^2)\left(1-\frac{4\mu_\pi{}^2}{M_\omega{}^2-M_\omega M+\mu_\pi{}^2}\right)\right]^{1/2} f'(\vec{q};M,\mu_\pi)|_{A=0}\,. \tag{B10}$$

4. $\phi\to\bar{K}K$

The same formula as in the $\rho\to 2\pi$ decay can be applied to this case with allowance for the appropriate masses. Since $M_\phi \simeq 2\mu_K$, we obtain an approximate formula

$$f_{(\phi\to K)}(\vec{q})=4F_\phi(2\vec{q})\,. \tag{B11}$$

*This work overlaps partially with the Ph.D. thesis of one of the authors (T.S.) and is supported in part by the National Research Council of Canada and the Department of Education of the Province of Quebec.

[1]J. Ballam *et al.*, Phys. Rev. D 4, 1946 (1971); P. L. Belenyi *et al.*, Nucl. Phys. B37, 621 (1972); B. M. Salzberg *et al.*, *ibid.* B41, 397 (1972); J. Bartsch *et al.*, *ibid.* B46, 356 (1972). See also J. Bartsch *et al.*, *ibid.* B19, 381 (1970); N. K. Yamdagni and S. Ljung, Phys. Lett. 37B, 117 (1971); P. S. Panvini *et al.*, Nucl. Phys. B39, 538 (1972); K. Boesebeck *et al.*, *ibid.* B40, 39 (1972); G. Yekutieli *et al.*, *ibid.* B40, 77 (1972); H. H. Bingham *et al.*, *ibid.* B41, 1 (1972); J. W. Lamsa *et al.*, *ibid.* B41, 338 (1972); D. Mettel, *ibid.* B42, 340 (1972); H. Johnstad *et al.*, *ibid.* B42, 558 (1972); C. Brankin *et al.*, *ibid.* B43, 1 (1972); R. Morse *et al.*, *ibid.* B43, 77 (1972); P. J. Davies *et al.*, *ibid.* B44, 344 (1972); H. H. Bingham *et al.*, Phys. Lett. 41B, 635 (1972); Many other papers are quoted in these papers.

[2]L. Van Hove, Phys. Lett. 28B, 429 (1969); Nucl. Phys. B9, 331 (1969).

[3]D. Amati, A. Stanghellini, and S. Fubini, Nuovo Cimento 26, 896 (1962); L. Bertocchi, S. Fubini, and M. Tonin, *ibid.* 25, 624 (1962); G. F. Chew and A. Pignotti, Phys. Rev. 176, 2112 (1968); Chan Hong-Mo, J. Łoskiewicz, and W. W. M. Allison, Nuovo Cimento 57A, 93 (1968); C. E. DeTar, Phys. Rev. D 3, 128 (1971); See also D. M. Tow, Phys. Rev. D 2, 154 (1970); J. Arafune and H. Sugawara, Prog. Theor. Phys. 48, 1652 (1972). These authors point out difficulties of the multiperipheral model.

[4]R. P. Feynman, Phys. Rev. Lett. 23, 1415 (1969); in *High Energy Collisions*, edited by C. N. Yang *et al.* (Gordon and Breach, New York, 1969). See also, E. L. Feinberg, Phys. Lett. 38B, 237 (1972). This author points out difficulties of the Feynman model.

[5]R. C. Hwa, Phys. Rev. Lett. 26, 1143 (1971); M. Jacob and R. Slansky, Phys. Rev. D 5, 1847 (1972); since the mass spectrum of produced fireball is essential in these models, a critical test can be done by the observation of missing-mass spectra. See, for example, Y. M. Antipov *et al.*, Phys. Lett. 40B, 147 (1972).

[6]T. Sasaki, Prog. Theor. Phys. 48, 198 (1972); 49, 1362 (1972).

[7]R. Hagedorn and J. Ranft, Nuovo Cimento Suppl. 6, 169 (1968).

[8](a) J. V. Allaby *et al.*, CERN Report No. 70-12, 1970 (unpublished); (b) H. J. Mück *et al.*, Phys. Lett. 39B, 303 (1972); (c) W. H. Sims *et al.*, Nucl. Phys. B41, 317 (1972); (d) R. S. Panvini *et al.*, Phys. Lett. 38B, 55 (1972); (e) L. G. Ratner *et al.*, Phys. Rev. Lett. 27, 68 (1971); (f) A. Bertin *et al.*, Phys. Lett. 38B, 260 (1972). (g) J. C. Sens, in *Proceedings of the Fourth International Conference on High Energy Collistons, Oxford, 1972*, edited by J. R. Smith (Rutherford High Energy Laboratory, Chilton, Didcot, Berkshire, England, 1972); (h) M. E. Law *et al.*, LBL Report No. LBL-80, 1972 (unpublished). Many experimental data are systematically listed in this.

[9]J. Benecke, T. T. Chou, C. N. Yang, and E. Yen, Phys. Rev. 188, 2159 (1969); T. T. Chou and C. N. Yang, Phys. Rev. Lett. 25, 1072 (1970).

[10]A. Bertin *et al.*, Phys. Lett. 41B, 201 (1972); M. G. Albrow *et al.*, Phys. Lett. 40B, 136 (1972).

[11]B. R. Webber, Phys. Rev. Lett. 27, 448 (1971).

[12]R. F. Amann, Phys. Rev. Lett. 26, 1349 (1972).

[13]S. Sakai, Prog. Theor. Phys. 48, 916 (1972); 49, 552 (1973). C. Boldrighini and L. Lusanna, Phys. Lett. 40B, 573 (1972).

[14]J. Ranft, Phys. Lett. 41B, 613 (1972).

[15]K. Kinoshita and H. Noda, Prof. Theor. Phys. 48, 1280 (1972). S. Yazaki, Phys. Lett. 43B, 225 (1973).

[16]R. N. Cahn, Phys. Rev. Lett. 29, 1481 (1972).

[17]H. Meyer and W. Struczinski, DESY Report No. DESY 72/40, 1972 (unpublished); T. Ferbel, Phys. Rev. Lett. 29, 448 (1972).

[18]L. Brink, W. N. Cottingham, and S. Nussinov, Phys. Lett. 37B, 192 (1971).

[19]N. Murai and K. K. Phua, Nuovo Cimento Lett. 5, 575 (1972); N. Murai and T. Sasaki, Prog. Theor. Phys. 50, 610 (1973).

[20]T. T. Chou, Phys. Rev. Lett. 27, 1247 (1971).

[21]T. Sasaki, Ph.D. thesis, University of Tokyo, 1972 (unpublished).

[22]F. Lurçat and P. Mazur, Nuovo Cimento 31, 140 (1964).

[23]M. Kugler and R. G. Roberts, Weizmann Institute of Science Report No. WIS 71/51 Ph., 1971 (unpublished).

[24]K. Schilling, P. Seyboth, and G. Wolf, Nucl. Phys. B15, 397 (1970).